

Development of Wrist Rehabilitation Device Using Extension Type Flexible Pneumatic Actuators with Simple 3D Coordinate Measuring System

W. Tian¹, Y. Suzuki¹, T. Akagi^{1*}, S. Dohta¹, W. Kobayashi¹, T. Shinohara¹, S. Shimooka² and Mohd Aliff³

¹Okayama University of Science, 1-1, Ridai-cho, Kita-ku, Okayama, 700-0005, Japan

Phone: +81-86-256-9786; Fax: +81-86-255-3611

²National Institute of Technology, Matsue College, 14-4, Nishiikuma-cho, Matsue, Shimane, 690-8518, Japan

³Malaysian Institute of Industrial Technology, Universiti Kuala Lumpur, Persiaran Sinaran Ilmu, Bandar Seri Alam, 81750 Johor, Malaysia

ABSTRACT – Rehabilitation devices have been developed to assist patients to recover from physical disabilities by using specific devices to do exercise, training and therapy. The purpose of this study is to develop a home-based rehabilitation device that is safe to use and without the requirement of a person in charge. In this study, a simple home-based wrist rehabilitation device that can give passive exercise on spherical orbit while patients hold its handles is proposed and tested. The device has two moving handling stages driven by six extension type flexible pneumatic actuators on two hemispherical acrylic domes. The device can give passive exercise for the upper limb by changing the relative position of the patient's hands. In this paper, the construction and operating principles of the tested device are described. A low-cost 3-dimensional coordinate measuring system using two wire-type linear potentiometers to control the position of the holding stages is also described. In addition, the tracking position control of the holding handles on a sphere is carried out. As a result, it can be found that the handling stage of the tested device can trace the desired orbit based on the coordinates measured from a 3-dimensional coordinate measuring system. It can be confirmed that the tested wrist rehabilitation device has the possibility to apply passive movements to the wrist along the desired orbit while patients hold its handles.

ARTICLE HISTORY

Received: 27th Jan 2021

Revised: 28th July 2021

Accepted: 1st Nov 2021

KEYWORDS

*Spherical actuator;
Extension type flexible
pneumatic actuator;
3D coordinate measuring
system;
Low-cost home-based
rehabilitation device;
Embedded controller*

INTRODUCTION

Nowadays in Japan, the number of people aged 60 years and older will keep increasing due to low fertility rates and high life expectancy [1]. Subsequently, systems to aid in nursing care [2] and to support the daily activities of the elderly and people with disabilities are highly required [3-6]. Rehabilitation devices help to restore the physical ability of patients for keeping their quality of life (QOL) [7-8]. A home-based rehabilitation device should hold several characteristics such as safe and easy to manage, cost-effective and flexible device, so there is no adversely impact on adherence to the patient [9]. In this study, we intend to develop a safe home-based rehabilitation device when patients hold it with both hands. In the case when the patient uses it at home by him/herself for voluntary rehabilitation exercise to keep moving area of joints, the device must be usable without any special knowledge and affordable in terms of cost. From a safety point of view, it is desirable that patients can easily release the device when they are afraid and in danger.

In the previous study, a flexible pneumatic spherical actuator using two flexible pneumatic cylinders was developed to offer rehabilitation motion for the upper limb by only changing the relative position of the patient's hands [10]. On the other hand, attitude control of portable rehabilitation devices using the flexible pneumatic spherical actuator, which can give passive exercises for patients while they were holding it by both hands were carried out. In this study, as a target motion using the desired device, 'a ball rolling exercise' that is well known as a voluntary rehabilitation exercise is assumed as shown in Figure 1.



Figure 1. Ball rolling exercise for wrist rehabilitation.

In the typical ball rolling exercise, the ball is rolled in each direction to give passive exercise to keep and increase the moving range of the wrist joint as a voluntary rehabilitation. Usually, a passive exercise leads to an increased moving area of diseased joints. As a concept of the proposed rehabilitation device, it is not to dramatically increase the moving area of the wrist joint; it is to keep the moving area after medical treatment by a physical therapist (PT) and to increase the moving area as an effect of passive exercise. The device only changes the holding position of the patient's hands automatically. And the patient can release the handle anytime. It means that the patient can adjust the applied force by themselves. Nevertheless, the previous spherical actuator has a low stiffness which will deform if it is impaired by the patient's reaction force. As an improvement, it is necessary to develop a device that holding stage can move on a rigid spherical surface and provide larger force to the patient's wrist as a passive exercise. In the next step, we aim to solve the problems of the previous spherical actuator, such as, too soft body, a narrow range of motion of the handling stages and the inability of the two holding handles to move independently. In detail, a device using two rigid hemispherical domes that can give a ball rolling exercise to both hands independently is proposed and tested. A low-cost, simple 3D coordinate measuring device that can be used to control the position of the stage on the spherical surface is also proposed and tested.

WRIST REHABILITATION DEVICE USING EXTENSION TYPE FLEXIBLE PNEUMATIC ACTUATORS

Extension Type Flexible Pneumatic Actuator

Figure 2 shows the view and schematic diagram of the tested extension type flexible pneumatic actuator (EFPA) [11]. Compared with McKibben type pneumatic artificial muscle, which can contract only about 25% of original, and the contracting force is decreasing according to the contraction. On the other hand, the EFPA can extend more than twice its original length, and equilibrium pulling force depends on the spring constant of the inner rubber tube and the initial pulling displacement. The EFPA consists of a silicone rubber tube covered with a bellows-type ruffled fabric sleeve made of nylon string and two acrylic end connectors with a supply port. The rubber tube has an inner diameter of 8 mm, an outer diameter of 10 mm and a length of 200 mm. The length of the actuator becomes 450 mm when 400 kPa supply pressure is applied. The operating principle of EFPA is as follows. When the supplied pressure is applied to the actuator, the inner rubber tube extends toward radial and longitudinal directions. As the bellows-type fabric sleeve can only deform toward longitudinal direction while preventing extension towards the radial direction, the actuator extends longitudinally. From the result of the preliminary experiment, it is confirmed that the actuator can extend more than 2.5 times the original length when the input pressure of 400 kPa is applied. The pushing force of the actuator while the actuator is being pressurised is small because of its flexibility. However, the pulling force in the case of decompression is huge. It is an elastic force of the rubber tube. The maximum pulling force is about 19.5 N for the actuator displacement of 250 mm.

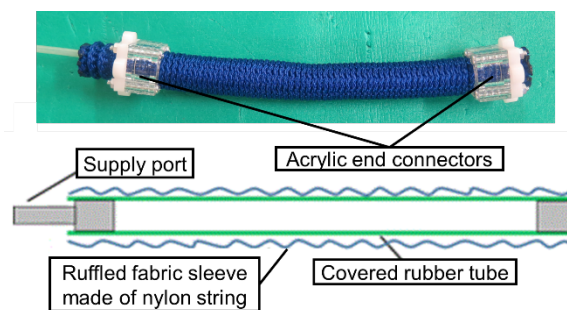


Figure 2. View and schematic diagram of the tested EFPA.

Wrist Rehabilitation Device using EFPAs

Figure 3 shows the construction of a tested wrist rehabilitation device using 6 EFPAs. The wrist rehabilitation device consists of two hemispherical acrylic domes with an outer diameter of 200 mm, 6 EFPAs with an original length of 250 mm, two acrylic handling stages, and the base stage. In the case of the proposed device, the device requires a larger moving area on a hemispherical surface. We need to adjust the stiffness of the handle in an equilibrium position. Therefore, we use EFPA in the device because EFPA has a large displacement and is easy to adjust the initial pulling force. Each handling stage is connected with three EFPAs that are arranged every 120 degrees from the centre of the hemisphere, and one set of three EFPAs for the handling stage is placed 60 degrees to another set of EFPAs from the centre of the hemisphere back-to-back. Another end of EFPA connected to each handling stage is set with the bottom of another hemispherical stage. Each handling stage is always pulled by three EFPAs. By using this method, the handling stage is able to move according to the spherical surface by adjusting the input pressure of three EFPAs. In addition, to stretch each EFPA until 315 mm from the original length of 250 mm in the neutral position, two hemispherical acrylic domes are placed with a distance of 400 mm. In order to prevent excessive elongation when the actuator is pressurised, restraints are also used in the centre part of the device and the bottom of the hemispherical acrylic domes. The total length and mass of the tested device are 650 mm and 3 kg, respectively.

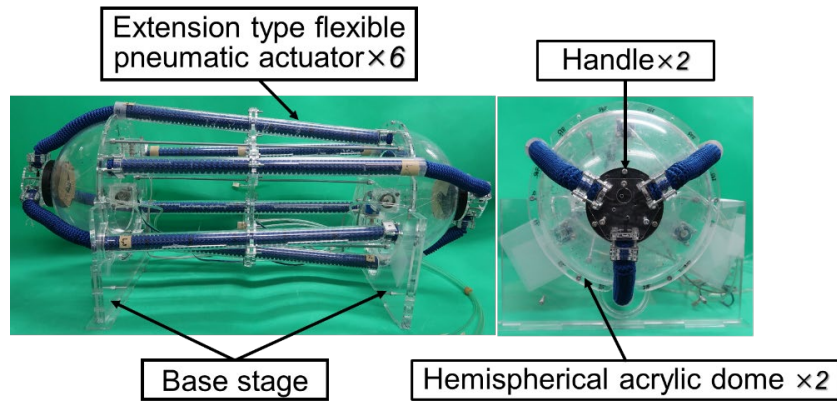


Figure 3. View of wrist rehabilitation device using EFPAs and acrylic domes.

Figure 4 shows the schematic diagram of the control system of the tested device. The system consists of the tested device, an embedded controller (Renesas electronics Co. Ltd., SH7125) and six quasi-servo valves. Each quasi-servo valve consists of two serial connected on/off valves (Koganei Co. Ltd., G010E-1). One valve is a switching valve to change supply or exhaust. The other is a PWM control valve which can adjust valve opening per time. The sequential position control of both handling stages in the tested device is as follows. By adjusting valve opening time to control the input flow rate to EFPA, the internal pressure of the EFPA will change. Meanwhile, the length of pressurised EFPA becomes longer, and the pulling force becomes smaller. Therefore, the position of holding stage is determined by the force balance of the three EFPAs acted on the stage. By this method, the position of both holding handles on hemispherical domes can be controlled.

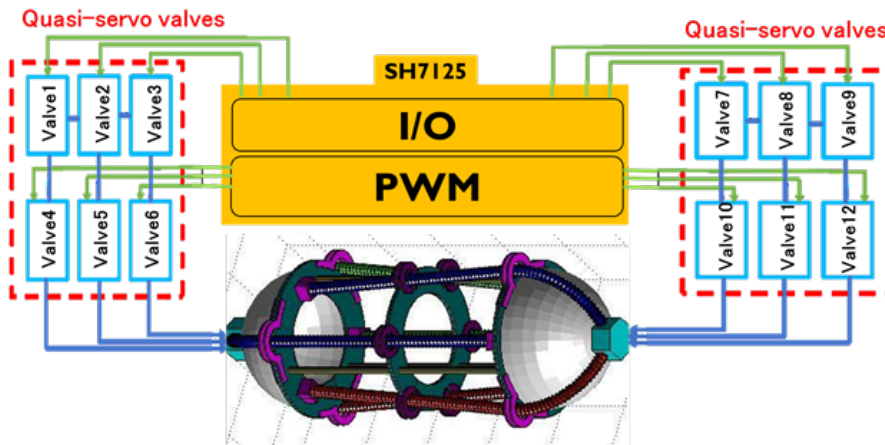
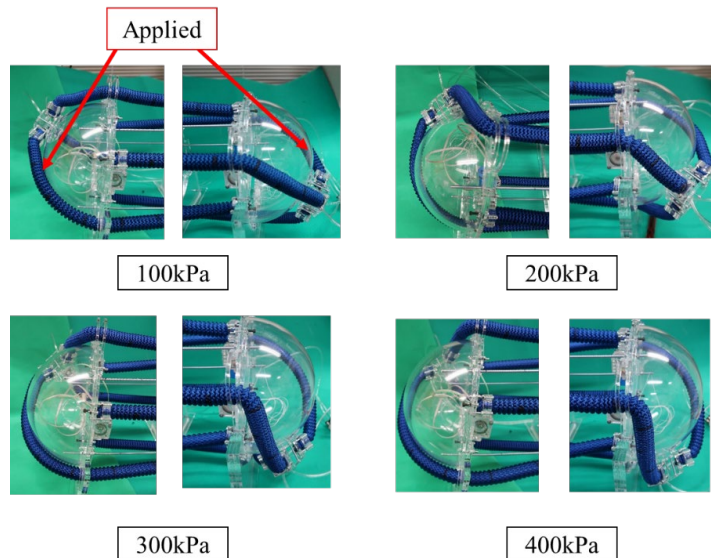
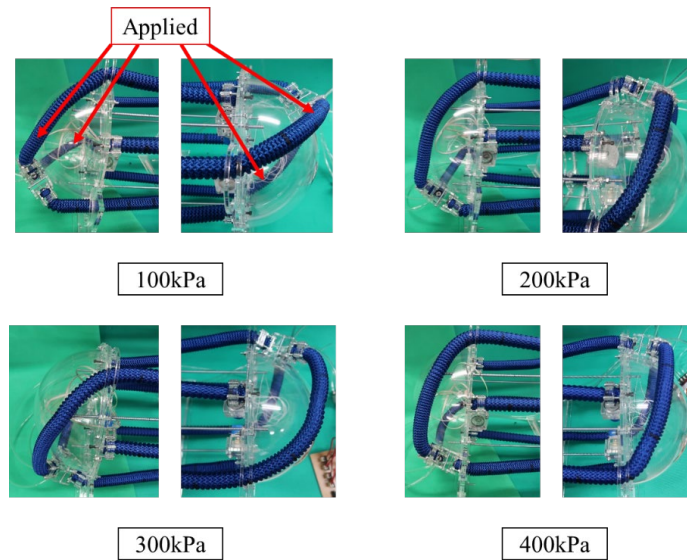


Figure 4. Schematic diagram of a control system of wrist rehabilitation device.



(a) The case when one EFPA is pressurised



(b) The case when two EFPAs are pressurised

Figure 5. View of movement of the tested device.

Figure 5(a) and 5(b) show the view of the movement of the device when supply pressure of 100, 200, 300, and 400 kPa are applied to one or two EFPAs in the drive, respectively. Both figures show that the position of handling stage can be adjusted according to the applied pressure in each EFPA. In addition, it can be confirmed that deflection of each EFPA does not occur when supply pressure is until 400 kPa by designing the initial length (natural length) under the condition of initial elongation (200%) of EFPA. As a result, it can be confirmed that the device can give passive exercise according to the spherical surface while the patient holds both handling stages. However, the tested system cannot control the position of handling stages precisely because there is no available position sensor that can measure 3D coordinate on the spherical surface on the market. As the next step, a low-cost 3D coordinate measuring system of holding the handle on the spherical dome will be proposed.

3D COORDINATE MEASURING SYSTEM ON SPHERICAL SURFACE

Model of the 3D Coordinate Measuring Device

In the proposed measuring system, the principle of triangulation was used as a method for measuring 3D coordinate on a spherical surface. Figure 6 shows the analytical model to measure 3D coordinate using the proposed system. Usually, to obtain 3D coordinates of a certain position, three lengths from different three points as base points are required. In the tested device, the handling stage always moves on the spherical surface with a certain radius r of 100 mm from the centre of sphere. Therefore, a 3D coordinate of measuring point can be obtained by only measuring two lengths from two different points to the measuring points. Based on this principle, in the model, two base points are set on the x and y axis with a distance d of 50 mm from the centre of the sphere. From a geometric relationship as shown in Figure 6, the following three equations of spheres from three points to the measuring point (x, y, z) can be obtained.

$$(r - w)^2 = x^2 + y^2 + z^2 \tag{1}$$

$$l_x^2 = (x - d)^2 + y^2 + z^2 \tag{2}$$

$$l_y^2 = x^2 + (y - d)^2 + z^2 \tag{3}$$

where, r , l_x , and l_y are the radius of sphere (100 mm) and length from positions on the x and y -axis to the measuring position, respectively, w is the gap of 14 mm from the spherical surface to measuring position, that is the binding point of three lines. From the intersection point of these spheres, the coordinate of measuring point (x, y, z) is given as follows.

$$x = \frac{(r - w)^2 - l_x^2 + d^2}{2d} \tag{4}$$

$$y = \frac{(r - w)^2 - l_y^2 + d^2}{2d} \tag{5}$$

$$z = \sqrt{(r - w)^2 - x^2 - y^2} \tag{6}$$

From Eq. (4) to (6), the coordinate of the handling stage can be obtained by measuring two distances l_x and l_y .

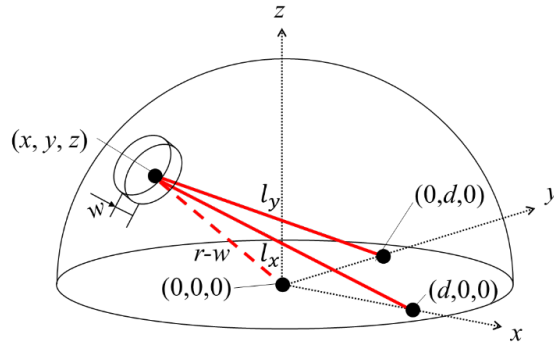


Figure 6. Model to measure 3D coordinate using the proposed system.

3D Coordinate Measuring Device

Figure 7 shows the tested 3D coordinate measuring device on the spherical surface. The device consists of the hemispherical acrylic dome, two wire type linear potentiometers placed on a round bottom plate, inner and outer guides of the handling stage. Two wires from potentiometers set on base points are connected to the bottom of the inner guide. Figure 8 shows the schematic diagram of inner and outer guides produced using a 3D printer (AFINIA Co. Ltd., H800+). Both guides have twelve holes. In each hole, a rectangular neodymium magnet with a dimension of 8×8×3 mm is installed. By attracting both inner and outer magnets, the inner guide can detect the movement of the outer guide. Figure 9 shows the view of the low-cost wire-type linear potentiometer.

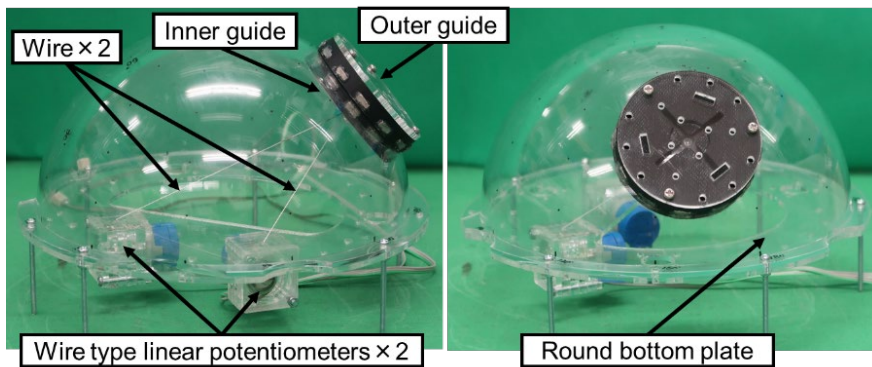


Figure 7. View of tested 3D coordinate measuring device.

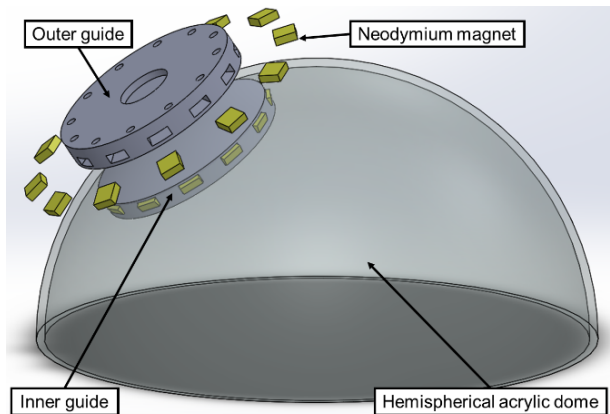


Figure 8. Schematic diagram of inner and outer guides in the tested device.

The left one in Figure 9 shows the whole device. The right one shows the device when the covered case of the wire spool is removed. The potentiometer consists of a helical potentiometer (Bourns Co. Ltd., 3590S-A26-104L) which can measure 10 times rotational angle connected with a clockwork wire spool and a polyethylene wire with a diameter of 0.32 mm. Both shafts of the clockwork wire spool and the potentiometer have connected each other. The prototype of the potentiometer was developed in the previous study. The prototype potentiometer has a measuring range of 0.7 m with a resolution of 0.74 mm. Therefore, the diameter of the wire spool is reduced to 7.0 mm (as shown in Figure 9) in order to fit the potentiometer range. As a result, the resolution of measuring the displacement of the improved potentiometer is 0.26 mm. In addition, the total material cost of the tested device, excluding the acrylic dome, is economical, which is only about USD 55.

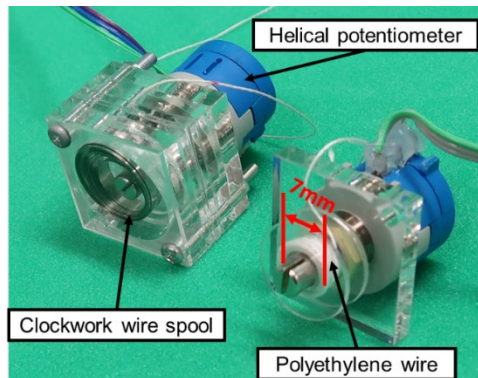


Figure 9. View of the wire-type linear potentiometer (Left: Whole device, Right: The covered case for wire spool is removed)

Measuring Results of 3D Coordinate Measuring Device

Figure 10 shows the measuring results using the tested 3D coordinate measuring device. In the experiment, the outer guide is set at a point on the sphere in the x - z plane and y - z plane. The setting position is marked on a spherical surface using a jig that can mark the position every 15 degrees in both azimuth angle on the x - y plane and elevation angle, as shown in Figure 11. The outer guide is set every 15 degrees between 30 and 150 degrees in elevation angle.

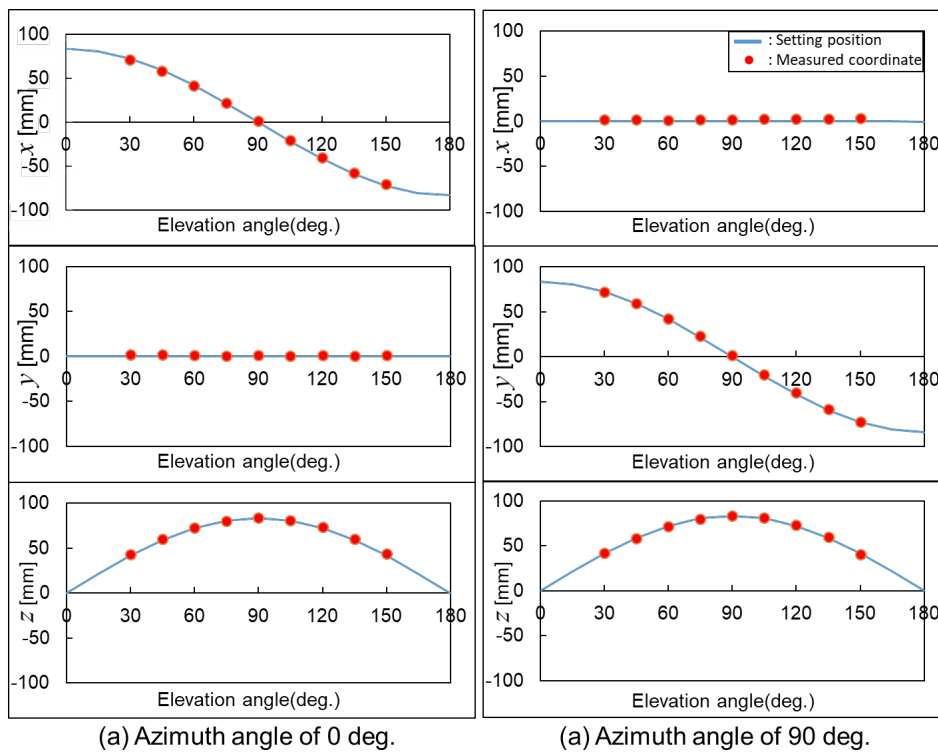


Figure 10. Measuring results using tested device in static condition.

Figure 10(a) shows the measuring results of the point on the sphere in the x - z plane, that is, the azimuth angle of 0 degree. Figure 10(b) shows the measuring result in the case of an azimuth angle of 90 degrees. In Figure 10, the horizontal axis of all graphs shows the elevation angle, and the blue lines and red symbols show the coordinate of setting position and the measured coordinate, respectively. The measured coordinate can be obtained by using the embedded controller through the A/D converter in the controller and the tested device based on the analytical model. From Figure 10, it can be seen that the measured coordinate can meet the set coordinate with the standard deviation of measuring error of x , y , and z coordinate are 1.29, 0.82 and 0.75 mm, respectively. It can also be confirmed that the tested device can measure the x and y coordinates with the standard deviation of measuring error of about 1.3 mm in static conditions.

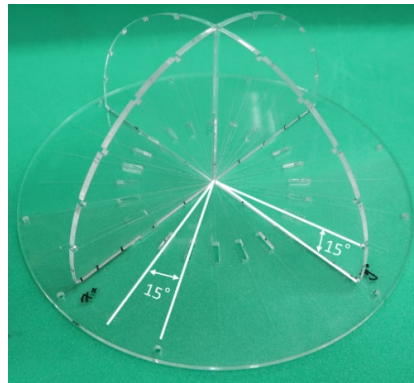


Figure 11. Jig to mark the position every 15 degrees in both azimuth angle and elevation angle.

Figure 12 shows the measuring result when the outer guide is moved on an arc horizontal to the x - y plane by hand. In the experiment, the arc with two heights of 42 and 59 mm are tested. In Figure 12, the blue line shows the setting arc that the outer guide traces by hand. Redline shows the measuring result. These measuring data are obtained through a serial communication port on a PC from the embedded controller. The difference between the setting position and measured position is caused by moving the outer guide by hand. From Figure 12, it can be found that the tested system can measure the position coordinate on a spherical surface in real-time. In the next step, we will integrate the 3D coordinate measuring device into the tested wrist rehabilitation device and perform the tracking control of the handling stage.

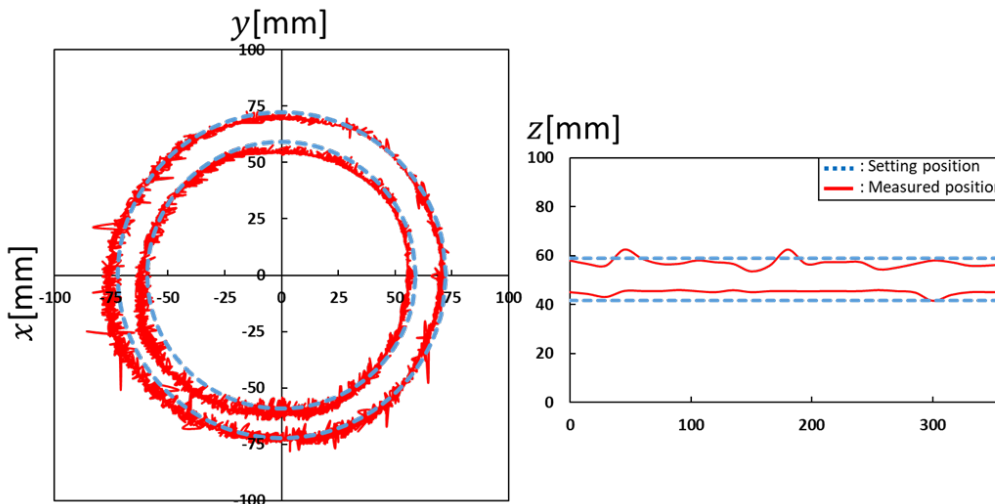


Figure 12. Measuring results using the tested device in dynamic conditions.

TRACKING CONTROL OF THE HOLDING HANDLE

Model for Tracking Control

In order to control the handling stage in the tested wrist rehabilitation device to trace the desired orbit, an analytical model to obtain the desired length and current length of each EFPA on the hemispherical dome from the target coordinates (x_r, y_r, z_r) and the measured coordinates (x, y, z) is required. Figure 13 shows the geometric relationship between the directional angle (angle with the x -axis in the x - z plane) α the elevation angle (angle with the x - z plane) β that from the coordinates on the hemispherical dome to the hemispheres center and the coordinates (x, y, z) of a point P. The coordinates (x, y, z) can be expressed by the following equation, where R is the radius of the hemisphere where the centre of EFPA exists.

$$x = R \cos \beta \cos \alpha \tag{7-1}$$

$$y = R \cos \beta \sin \alpha \tag{7-2}$$

$$z = R \sin \beta \tag{7-3}$$

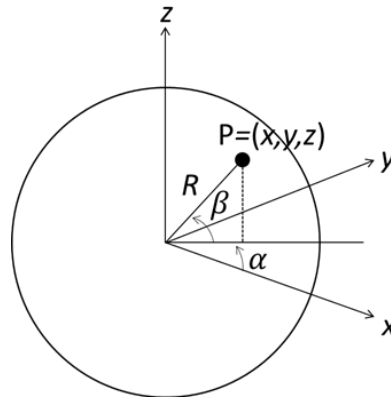


Figure 13. Geometric relationship between the direction angle α , the elevation angle β and the coordinates P on the hemisphere.

The geometric relationship of the length of the arc between any two points P_1 and P_2 is shown in Figure 14. The arc length L between the point P_1 (radius R , direction angle α_1 , elevation angle β_1) on the hemisphere and the point P_2 (radius R , direction angle α_2 , elevation angle β_2) that on the equator of the hemisphere (x - y plane) can be obtained by the following equations.

$$L_i = R\theta_i \quad (i = 1, 2, 3, 4, 5, 6) \tag{8}$$

$$\theta_i = 2 \sin^{-1} \left(0.5 \sqrt{X^2 + Y^2 + Z^2} \right) \tag{9}$$

where θ_i is the central angle of the arc between the two points, as shown in Figure 14. In addition, X , Y , and Z in Eq. (9) are expressed by the following equations.

$$X = \cos \beta_2 \cos \alpha_2 - \cos \beta_1 \cos \alpha_1 \tag{10-1}$$

$$Y = \cos \beta_2 \sin \alpha_2 - \cos \beta_1 \sin \alpha_1 \tag{10-2}$$

$$Z = \sin \beta_2 - \sin \beta_1 \tag{10-3}$$

Using these equations, the length L of the arc of each EFPA on the hemispheres can be obtained.

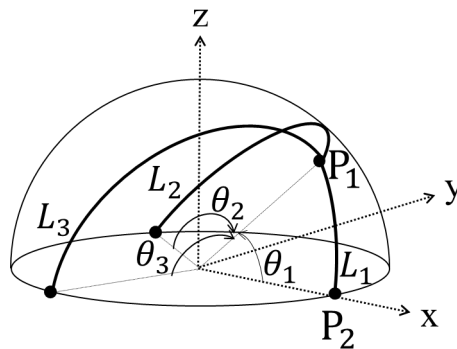


Figure 14. Model of the left hemisphere of the tested device.

First, we consider the left hemisphere of the tested device. Here, the point $P_1 (R, \alpha, \beta)$ on the hemisphere and P_2 on the equator are $(R, 0, 0)$, so that $\alpha_1 = \alpha, \beta_1 = \beta, \alpha_2 = 0, \beta_2 = 0$. Substituting each parameter into the equation, the central angle of the arc and the arc length can be expressed by Eq. (8) to Eq. (10); the central angle θ_1 of the arc L_1 can be expressed by the following equation.

$$\theta_1 = 2 \sin^{-1} \frac{1}{2} \sqrt{2 - 2 \cos \beta \cos \alpha} \tag{11-1}$$

In the same way, the central angle θ_2, θ_3 of the arc can be expressed by the following equations.

$$\theta_2 = 2 \sin^{-1} \frac{1}{2} \sqrt{2 + \cos \beta (\cos \alpha - \sqrt{3} \sin \alpha)} \tag{11-2}$$

$$\theta_3 = 2 \sin^{-1} \frac{1}{2} \sqrt{2 + \cos \beta (\cos \alpha + \sqrt{3} \sin \alpha)} \tag{11-3}$$

Also, the central angle $\theta_4, \theta_5, \theta_6$ of the arc and on the right hemisphere of the tested device can be expressed by the following equations.

$$\theta_4 = 2 \sin^{-1} \frac{1}{2} \sqrt{2 + 2 \cos \beta' \cos \alpha'} \tag{11-4}$$

$$\theta_5 = 2 \sin^{-1} \frac{1}{2} \sqrt{2 + \cos \beta' (\cos \alpha' - \sqrt{3} \sin \alpha')} \tag{11-5}$$

$$\theta_6 = 2 \sin^{-1} \frac{1}{2} \sqrt{2 - \cos \beta' (\cos \alpha' + \sqrt{3} \sin \alpha')} \tag{11-6}$$

where α' is the direction angle (angle with the x -axis in the x - z plane) and β' is the elevation angle (angle with the x - z plane) that from the coordinates on the right hemispherical dome to the hemispheres center.

By using these equations, the arc length on the hemispherical dome from the target coordinates (x_r, y_r, z_r) and the measured coordinates (x, y, z) to the x - z plane can be determined. In a word, lengths of the each EFPA can be determined.

Tracking Position Control and Result

Figure 15 shows the schematic diagram of the position control system using the tested rehabilitation device. The system consists of the tested rehabilitation device with two 3D coordinate measuring devices, six quasi-servo valves, and an embedded controller (Renesas Electronics Co. Ltd., SH7125). The position control of both handling stages is done as follows. First, the target length of each EFPA is calculated based on the model mentioned above from the desired coordinate by the embedded controller. The embedded controller gets output voltage from two potentiometers from each 3D coordinate measuring device through an A/D converter. Then, both current coordinates of handling stages on the left and right hemispherical domes are obtained based on the model and these AD values. The current length of the EFPA is also calculated from these obtained coordinates. From the error between the target length L_{ir} and the current length L_i of each EFPA, the quasi-servo valve is driven based on the following proportional control scheme.

$$u_i = k_p (L_{ir} - L_i) \tag{12}$$

$$D_i = u_i + 22.5 \tag{13}$$

where, k_p is the proportional gain. u_i and D_i are the control input and input duty ratio for the PWM control valve in each quasi-servo valve, respectively. 22.5% in Eq. (13) means the duty ratio corresponding to the dead zone when the on/off valve is driven at a PWM period of 10 ms. The switching on/off valve in the quasi-servo valve is switched to the supply or exhaust states according to a positive or negative value of control input as follows.

$$\left. \begin{array}{l} \text{supply} \quad (u_i > 0) \\ \text{exhaust} \quad (u_i < 0) \\ D_i = 0 \quad (u_i = 0) \end{array} \right\} \tag{14}$$

The proportional gain $k_p = 30 \text{ \%}/\text{mm}$ for supply ($u_i > 0$), and the proportional gain $k_p = \infty$ that means duty ratio is always 100 % for exhaust ($u_i < 0$) were used. It is because the exhaust flow rate is lower than the supply flow rate due to the physical phenomenon of air flow, such as a choked flow. In the case of this rehabilitation device, the tensile force of the EFPA is used to move the holding handle, and this control law is used to maximise the tensile force.

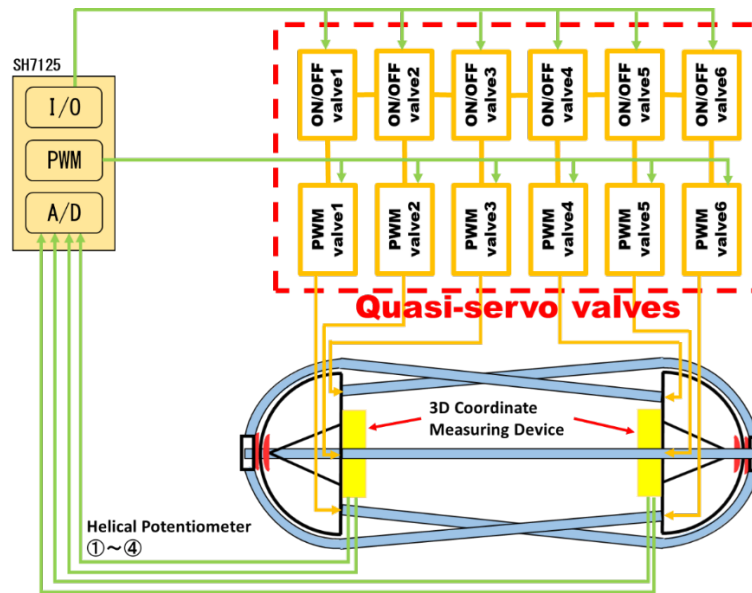


Figure 15. Schematic diagram of position control system using the tested device.

In position control, since the friction between the guide and the acrylic dome affects the control performance, a sliding-type guide with ball-shaped neodymium magnets was used. Figure 16 shows the schematic diagram of the inner construction of the sliding type guide. Compared with the previous guide, ball-shaped neodymium magnets with a diameter of 8 mm were used instead of rectangular magnets. By using the guide, the sliding frictional force can be reduced from 10 N to 5 N.

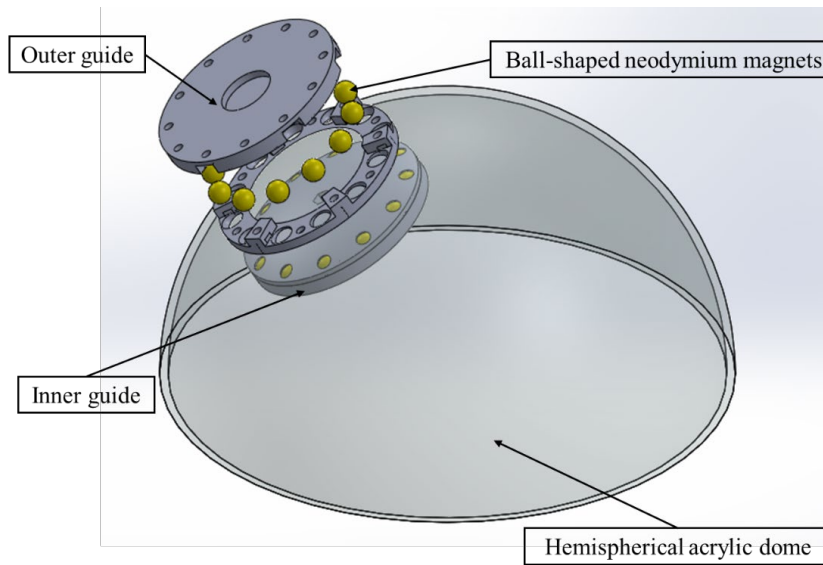


Figure 16. Schematic diagram of the guides of the device tested after improvement.

Figure 17(a) and 17(b) show results of tracking position control of both handling stages on left and right sides, respectively. In both figures, the upper figure shows the result of the x - y coordinate plane and the lower figure shows the z coordinate. In the experiment, the hemisphere surface with a constant height from the base was given as a target trajectory. In detail, the desired direction angle α was changed from 0 to 360 deg with a period of 60 s with constant elevation angle $\beta = 60$ deg. In Figure 17, blue and orange lines show the target trajectory and the controlled position of handling stages, respectively. From the X-Y results in Figure 17, vibrations are found in the graph. In the case when the patient holds the handle, the vibration can be reduced by the load. We also checked the video of the experiment when there was no load, and we did not find such a large vibration. Therefore, the vibration is caused by the noise in the dynamic measurement by using the 3D coordinate measuring device and a tiny embedded controller. Figure 18 shows the transient response of the controlled length of each EFPA.

In Figure 18, the vertical axis shows the arc length of each EFPA on the hemispherical dome, and the horizontal axis shows time. The dashed and solid lines indicate the desired length and the controlled length (actual length), respectively. From Figure 18, it can be seen that each EFPA can follow the target length relatively well. The standard deviation of the error of each EFPA (L_1 to L_6) with respect to the target length is 0.82, 0.66, 0.12, 5.04, 3.30, and 1.48 mm, respectively. As a result, it can be concluded that the wrist rehabilitation device whose handling stages can trace the target trajectory

can be realised. By providing the suitable desired orbit for wrist rehabilitation, the device can provide a suitable passive exercise to patients while they are only holding both handling stages in the device.

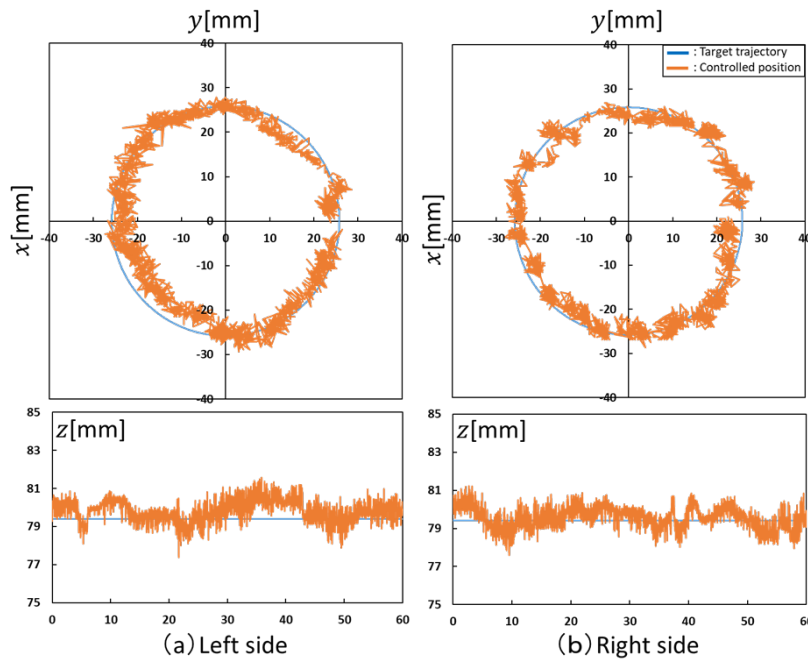


Figure 17. The results of tracking position control of both.

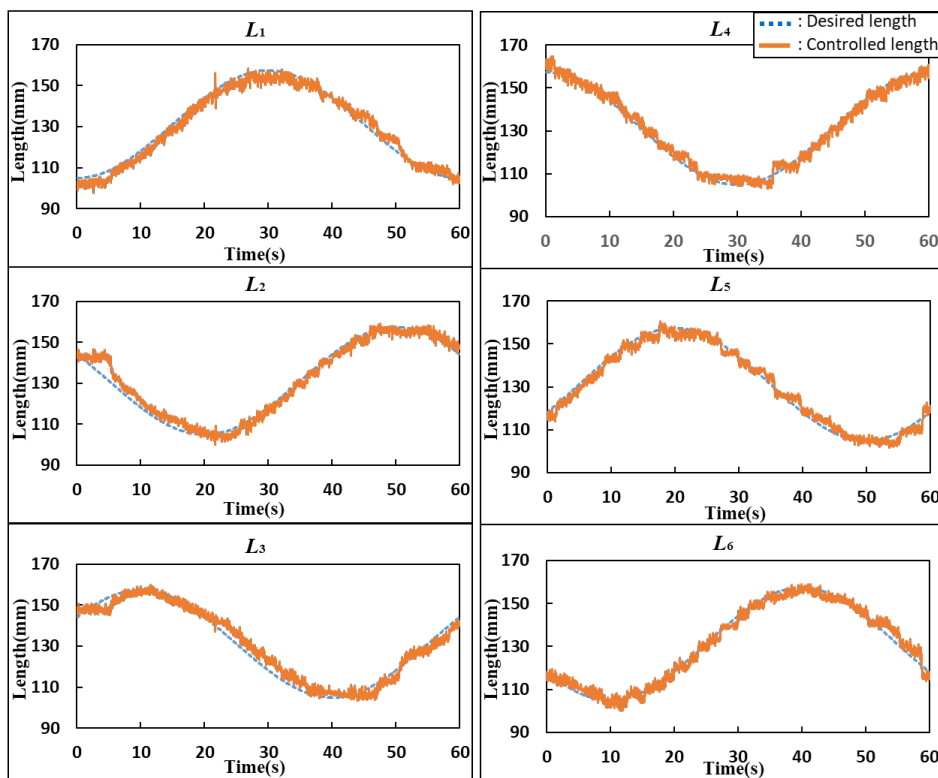


Figure 18. Transient response of controlled length of each EFPA.

CONCLUSION

This study aims to develop a home-based wrist rehabilitation device that can realise passive exercise such as a typical ball rolling exercise while patients are only holding moving stages in the device. It can be summarised as follows.

- i. As a home-based rehabilitation device, the wrist rehabilitation device using six extension type flexible pneumatic actuators (EFPAs) and acrylic hemispherical domes that its handling stages can be driven independently on a rigid hemispherical surface is proposed and tested. The sequence driving system using on/off valves and an

- embedded controller was also developed. As a result, the tested device can give passive exercise according to the spherical surface while the patient only holds both handling stages.
- ii. In order to measure the position of the handling stage on a spherical surface, a 3D coordinate measuring system that consists of two wire type linear potentiometers, inner and outer guides with magnets and an embedded controller is proposed and tested. The analytical model of the tested measuring system based on the principle of triangulation is also proposed. As a result, it can be confirmed that the tested system can measure the x and y coordinates of the handling stage with the standard deviation of measuring error of about 1.3 mm.
 - iii. In order to realise tracking position control of handling stages in the device, a model to calculate the length of each EFPA on the hemispherical dome is also proposed and tested. As a result, it can be concluded that the tested device can trace the target trajectory within a standard deviation error of 1.5 mm based on the model.

As future work, the suitable desired orbit using the tested device is going to be investigated by cooperating with physical therapists and occupational therapists. In addition, we are going to realise the intelligent rehabilitation system with force feedback. If we can know the reaction force exactly from the patient, we are also going to consider the suitable control scheme.

ACKNOWLEDGEMENT

This study was supported by the Education Ministry of Japan through a Financial Assistance Program for QOL Innovative Research (2012-2016) and a Grant-in-Aid for Scientific Research (C) (Subject 16K06202 & 19K04265).

REFERENCES

- [1] The 2rd year of Reiwa era version of the White Book of the Ageing Society (all version), 2020 [Online]. Available: https://www8.cao.go.jp/kourei/whitepaper/w-2020/zenbun/02pdf_index.html [Accessed: Oct. 25, 2021]
- [2] C. Ishii and K. Yoshida, "Improvement of a lightweight power assist suit for nursing care," *Int. J. Eng. Technol.*, vol. 11, no. 4, pp. 256-261, 2019.
- [3] M. Kashima *et al.*, "Development of assist suit for squat lifting support considering gait and quantitative evaluation by three-dimensional motion analysis," *J. Robot. Mechatron.*, vol. 32, no. 1, pp. 209-219, 2020.
- [4] N. Mir-Nasiri and H.S. Jo, "Energy efficient autonomous lower limb exoskeleton for human motion enhancement," *Int. J. Mech. Mechatron. Eng.*, vol. 10, No. 8, pp.1504-1511, 2016.
- [5] M. Takada *et al.*, "Active cloth fabricated by a flat string machine and its application to a safe wheelchair system," *J. Robot. Mechatron.*, vol. 32, no. 5, pp. 1010-1018, 2020.
- [6] H. Taniguchi *et al.*, "Realistic and highly functional pediatric externally powered prosthetic hand using pneumatic soft actuators," *J. Robot. Mechatron.*, vol.32, no. 5, pp. 1034-1043, 2020.
- [7] C. Zhang *et al.*, "Kinematic design of a footplate drive mechanism using a 3-DOF parallel mechanism for walking rehabilitation device," *J. Adv. Mech. Des. Syst. Manuf.*, vol.12, no.1, JAMDSM0017, 2018.
- [8] K. Shiota *et al.*, "Enhanced Kapandji test evaluation of a soft robotic thumb rehabilitation device by developing a fiber-reinforced elastomer-actuator based 5-digit assist system," *Rob. Auton. Syst.*, vol. 111, pp. 20-30, 2019.
- [9] Y. Nagata, *Soft actuators -forefront of development*. Tokyo: NTS Ltd, pp. 291-335, 2004.
- [10] Y. Matsui *et al.*, "Development of flexible spherical actuator with 3D coordinate measuring device," *J. Flow Control Meas. Visual.*, vol. 6, no.2, pp. 96-98, 2018.
- [11] W.H. Tian, *et al.*, "Development of a tetrahedral-shaped soft robot arm as a wrist rehabilitation device using extension type flexible pneumatic actuators," *J. Robot. Mechatron.*, vol. 32, no. 5, pp. 931-938, 2020.